Rev. 1
September 18, 1995

Dresden Unit 2
Core Spray Flaw Evaluation Report

September 18, 1995

ATTACHMENT A

CORE SPRAY FLAW EVALUATION REPORT
REVISION 1

Dresden Unit 2
Core Spray Flaw Evaluation Report

REPORT TABLE OF CONTENTS

		Page
1.0	INTRODUCTION	5
2.0	DESCRIPTION OF INDICATIONS	8
3.0	MATERIALS EVALUATION	17
4.0	LOAD DEFINITIONS AND LOAD COMBINATIONS	19
5.0	CORE SPRAY PIPING MODELLING AND ANALYSIS	23
6.0	FINITE ELEMENT MODELLING AND ANALYSIS	27
7.0	FLAW EVALUATIONS	33
8.0	LEAKAGE FLOW EVALUATIONS	44
9.0	CORE SPRAY SYSTEM LOCA EVALUATION	48
10.0	SUMMARY AND CONCLUSIONS	50
11.0	REFERENCES	52

LIST OF TABLES

Table		Page
2.1	Summary of Flaw Lengths	16
6.1	Normalized Load Distribution on the Thermal Sleeve Collar	32
7.1	Flaw Evaluation Stress Values	35
7.2	Flaw Evaluation Results	37
7.3	Flaw Evaluation Sensitivity Analysis - Stress Values	43
7.4	Flaw Evaluation Sensitivity Analysis - Results	43

LIST OF FIGURES

Figure		Page
1.1	Core Spray Piping Inside the RPV Annulus	7
2.1	Core Spray A-Loop 290° Upper Sparger Inlet Thermal Sleeve	9
2.2	Core Spray B-Loop 260° Lower Sparger Inlet Thermal Sleeve	10
2.3	Ultrasonic Test Examination Area and Flaw Location Elbow Weld 4	13
2.4	Ultrasonic Testing Examination Area and Flaw Location Thermal Sleeve Weld 2	14
2.5	Ultrasonic Testing Examination Area and Flaw Location Thermal Thermal Sleeve Weld 18	15
5.1	Core Spray Piping Model	25
6.1	Three Dimensional View of FEA Model	28
6.2	Vertical Cross Section of FEA Model	29
7.1	Cross Section of Flawed Pipe Section	38
7.2	Moment - Rotation Angle Relationship	40
8.1	Leakage Rate at a Differential Pressure of 47psi	46
8.2	Leakage Rate at a Differential Pressure of 64psi	47

1.0 INTRODUCTION

The portion of the core spray line addressed by this condition assessment is located in the reactor pressure vessel (RPV) annulus of Dresden Unit 2. The RPV annulus portion of the core spray lines consists of two symmetrical loops with RPV penetrations at the 5° and 185° azimuths. These two loops feed the two upper and two lower core spray spargers through four core shroud penetrations. A representative example of the RPV annulus portion of the core spray system is illustrated in Figure 1.1.

On July 11, 1995, Dresden Site Engineering initiated the D2R14 planned in-vessel visual inspection (IVVI). The inspection was planned as a thorough rebaselining inspection of the condition of some of the reactor vessel internals, using the enhanced visual inspection techniques similar to those first used at Dresden Station during the Unit 3 1994 refueling outage and now adopted as the industry standard for reactor vessel core shroud inspections. On July 12, 1995, cracking was detected in the core spray piping by the Dresden Site Engineering inspectors.

Crack like indications were observed at three locations on the core spray downcomers. One each in the "B" loop lower sparger inlet elbow and thermal sleeve collar and one in the "A" loop upper sparger inlet thermal sleeve collar. The elbow is made of stainless steel and is 6 inches in diameter. The affected piping is located in the reactor annulus between the reactor vessel wall and the core shroud wall. The elbow is not part of the reactor coolant pressure boundary nor is it part of the core shroud. The thermal sleeve collars are attached to the shroud on one side and to the 6 inch diameter core spray line on the other side. The thermal sleeve collars have the function of providing a leakage seal between the pipe and the annulus as shown in Figures 2.1 and 2.2. All three of the indications are circumferential.

The main analytical approach used here to justify continued operation is a limit load analysis which only requires primary loads in the evaluation. However, additional sensitivity studies were also performed using simplified elastic-plastic fracture mechanics, by means of Z factors, in which secondary loads from the thermal, seismic and LOCA events are included. The loads used to evaluate these flaws were developed from a piping analysis model and a three dimensional finite element model of the core shroud thermal sleeve penetration. This report provides the analysis details including the assessment criteria, design inputs and results for the various evaluations performed for the core spray cracking identified during the D2R14 in-vessel visual inspections. Section 2 of this report provides a summary of the method and extent of the examinations performed as well as the detailed definition of the

indications identified. Section 3 provides the materials evaluation with an assessment of the root cause and definition of material properties and crack growth rate for use in the flaw evaluation. The definition of the loading cases and load combinations used are provided in Section 4. A detailed description of the core spray line modeling and analyses along with a summary of the results is provided in Section 5. Section 6 provides a description of the finite element analysis (FEA) performed on the thermal sleeve collar, including descriptions of the modeling, the analysis and the results. The flaw and leakage flow evaluations are described in sections 7 and 8, respectively. Section 9 provides a description of the core spray system LOCA evaluation. A summary of the results and conclusions is provided in Section 10, while the references are presented in Section 11.

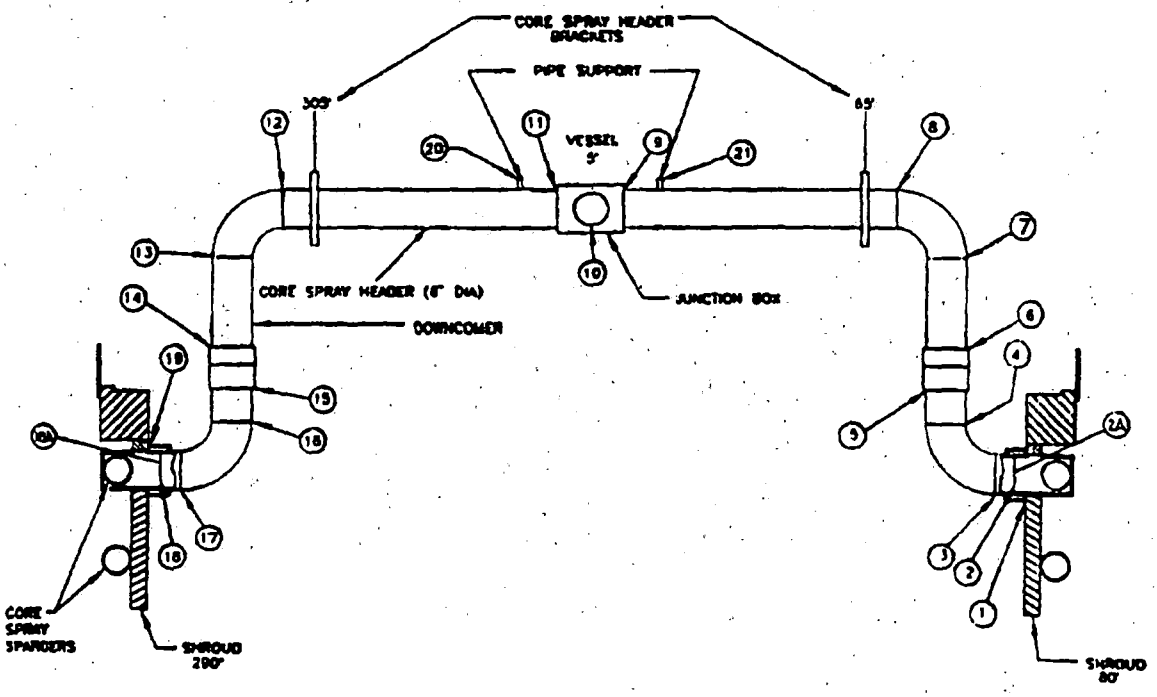

Figure 1.1 Core Spray Piping in the RPV Annulus

2.0 DESCRIPTION OF INDICATIONS

2.1 Visual Inspections

An enhanced visual inspection (0.5 mil wire resolution) was performed during the D2R14 refuel outage, of each of the internal core spray piping header and downcomer welds. Crack indications were identified in three locations. A description of the flaws identified, along with the length of each flaw as determined by visual sizing techniques is provided below. It should be noted that the flaws were very tight and that a best effort approach was used to visually size the lengths and locations of the flaws. The crack orientations as described below are given from the perspective of standing at the RPV and facing the shroud.

2.1.1 Core Spray Loop A 290° Upper Sparger Inlet Thermal Sleeve Collar

The flaw is located in the thermal sleeve collar at approximately 0.5 inches back from the face of the collar adjacent to weld 18 (See Figure 2.1). The flaw is located between the 4:00 position and 5:00 position with an estimated total length of 2 inches.

2.1.2 Core Spray Loop B 260° Lower Sparger Inlet Thermal Sleeve Collar

The flaw is located in the thermal sleeve collar at approximately 0.5 inches back from the face of the collar adjacent to weld 2 (See Figure 2.2). The flaw is located between the 9:00 and the 10:00 position. Multiple branching was observed at the 9:00 position. The total flaw length (including the branching) is estimated to be 2.25 inches.

2.1.3 Core Spray Loop B 260° Lower Sparger Inlet Elbow

The flaw is located in the elbow side of the pipe to elbow weld, within the heat affected zone of weld 4 (See Figure 2.2). The flaw is located between the 9:30 position and the 12:00 position. Significant branching was observed within the length of the flaw. The total flaw length is estimated to be 3.5 inches.

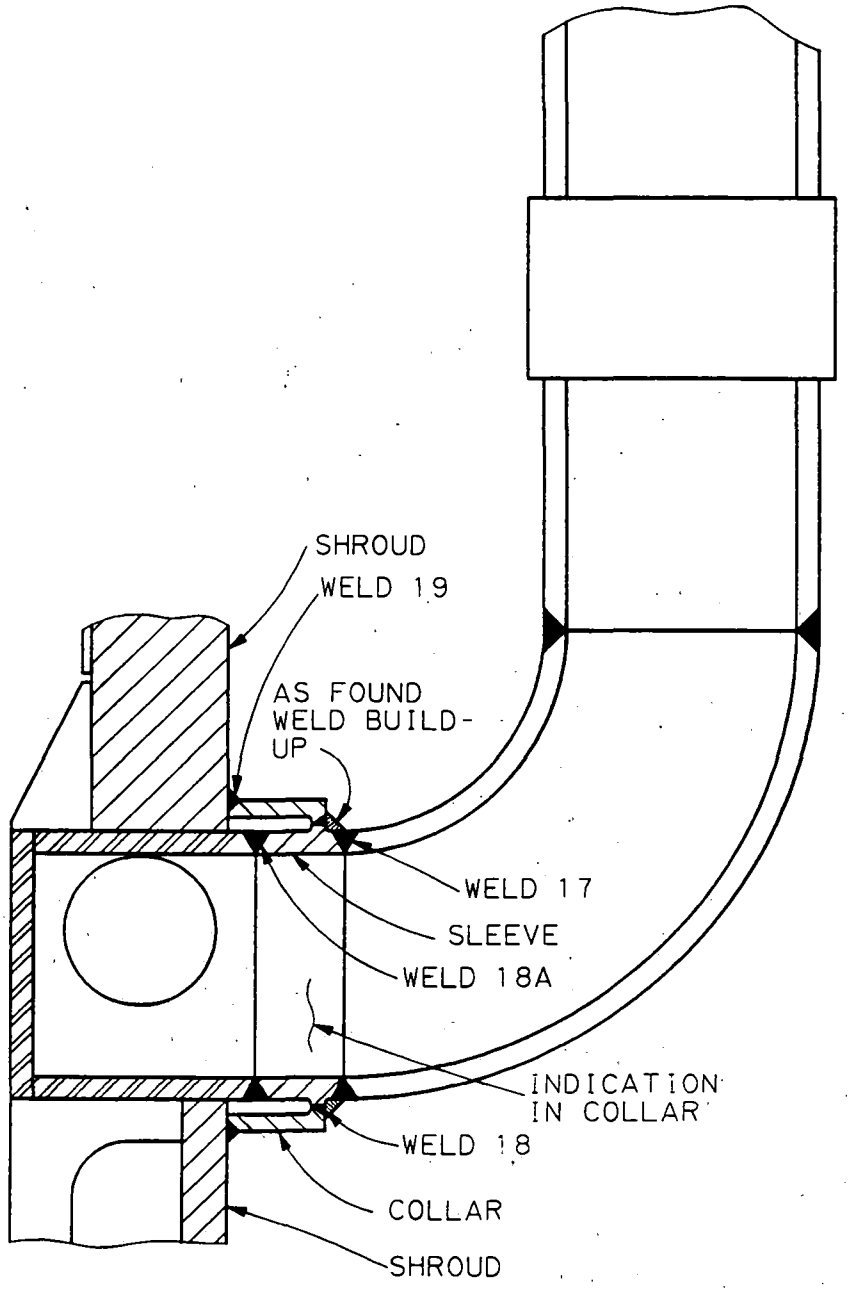

Figure 2.1 Core Spray A-Loop 290° Upper Sparger Inlet Thermal Sleeve

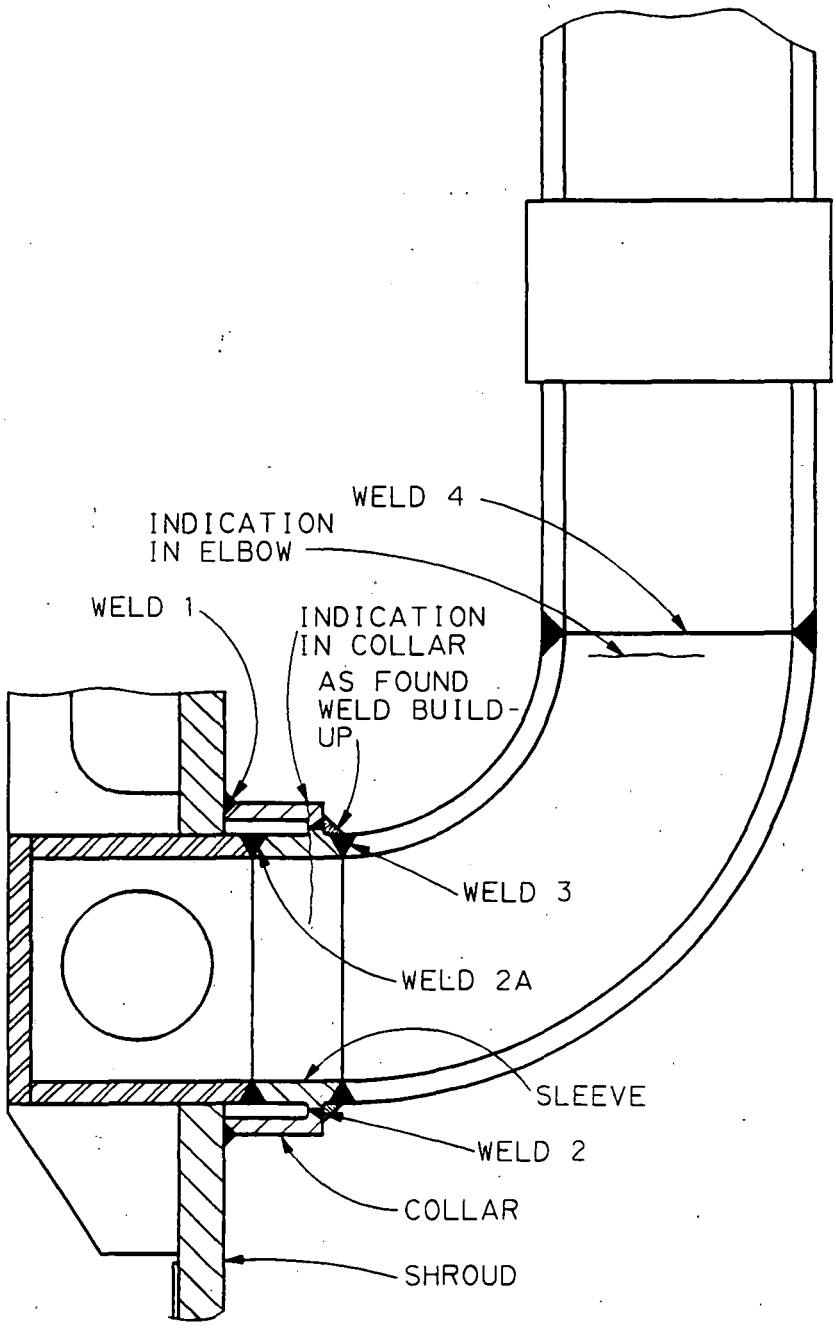

Figure 2.2 Core Spray B-Loop 260° Lower Sparger Inlet Thermal Sleeve & Elbow

2.2 Ultrasonic Examination

The purpose of this ultrasonic (UT) examination was to characterize the length of the OD connected flaws which were first detected with an enhanced visual inspection and to detect any ID connected flaws which may be less than through wall in depth. The ultrasonic technique used for the examination of the visually detected flaws in the core spray piping was developed by GE and qualified using mockups. The UT technique and qualification process was independently reviewed by EPRI (Reference 4) and ComEd and is described briefly below.

The ultrasonic probes were attached to a semicircular fixture on a long pole. The fixture was manually positioned on the pipe. When examining the thermal sleeve collar at the shroud penetration, the back of the fixture was pressed against the shroud wall, with the sound beams directed away from the shroud toward the end of the sleeve. Inside-surface and outside-surface circumferential notches in the mockup were located 0.5 inch from the end of the sleeve (the same position as the visual indications at Dresden). The smallest notches, one each on the inside surface and outside surface, were 0.020 inch deep. Two probes were evaluated, a Sigma SDA4 2(.51x27) 80L fd10 and an RTD TRCr2 2(7x12) SA3°. The Sigma probe's performance on the mockup was clearly superior. Using the Sigma probe, all notches produced strong ultrasonic responses and effective coupling was easier to achieve. It was this probe that was used in the remainder of the mockup tests and in the field examinations.

The qualifications using the probes and mockups established that the technique is effective in determining the presence or absence of cracking. This technique also proved to be useful in verifying the endpoints of the visually-detected flaws, whether the flaw extremities were connected to the inside or the outside surface. However, it was not practical to measure crack depth or to positively distinguish inside-surface from outside-surface cracking because of the thin wall. Provided below and in Figures 2.3, 2.4 and 2.5 is a description of the results of the UT examination.

2.2.1 Core Spray Loop A 290° Upper Sparger Inlet Thermal Sleeve Collar

The enhanced visual examination detected a crack in the thermal sleeve collar, approximately 0.5 inches back from the face of the collar, between the 4:00 and 5:00 position with an estimated total length of 2 inches. The UT examination of this thermal sleeve, Figure 2.3, confirmed the presence of the crack and indicated it to be ID connected. The crack was identified by UT to extend from approximately 4:00 to 5:00 (same location as OD visual examination) with an estimated length of 2 inches. The UT examination covered 360° of the thermal sleeve circumference, with no additional flaw indications detected.

2.2.2 Core Spray Loop B 260° Lower Sparger Inlet Thermal Sleeve Collar

The enhanced visual examination detected a crack in the thermal sleeve collar at approximately 0.5 inches back from the face of the collar, between the 9:00 and 10:00 positions with an estimated flaw length of 2.25 inches. The UT examination of this thermal sleeve, Figure 2.4, confirmed the presence of this crack and indicated it to be ID connected. The crack was identified by UT to extend from approximately 9:00 to 11:30 with an estimated length of 5.5 inches. The UT examination also detected another crack indication (believed to be ID connected) that was not visually detected. The crack was identified by UT to extend from approximately 1:30 to 3:00 with an estimated length of 3 inches. The UT examination covered 360° of the thermal sleeve, with no additional flaw indications detected.

2.2.3 Core Spray Loop B 260° Lower Sparger Inlet Elbow

The enhanced visual examination detected a crack in the pipe to elbow weld, within the heat affected zone of weld 4, between the 9:30 and 12:00 position with an estimated length of 3.5 inches. The UT examination of this elbow weld, Figure 2.5, confirmed the presence of the crack and indicated it to be ID connected. The crack was identified by UT to extend from approximately 9:30 to 11:30 (same approximate location as OD visual examination) with an estimated length of no more than 3.5 inches. The UT examination covered approximately 270° of the elbow weld circumference, with no additional flaw indications detected.

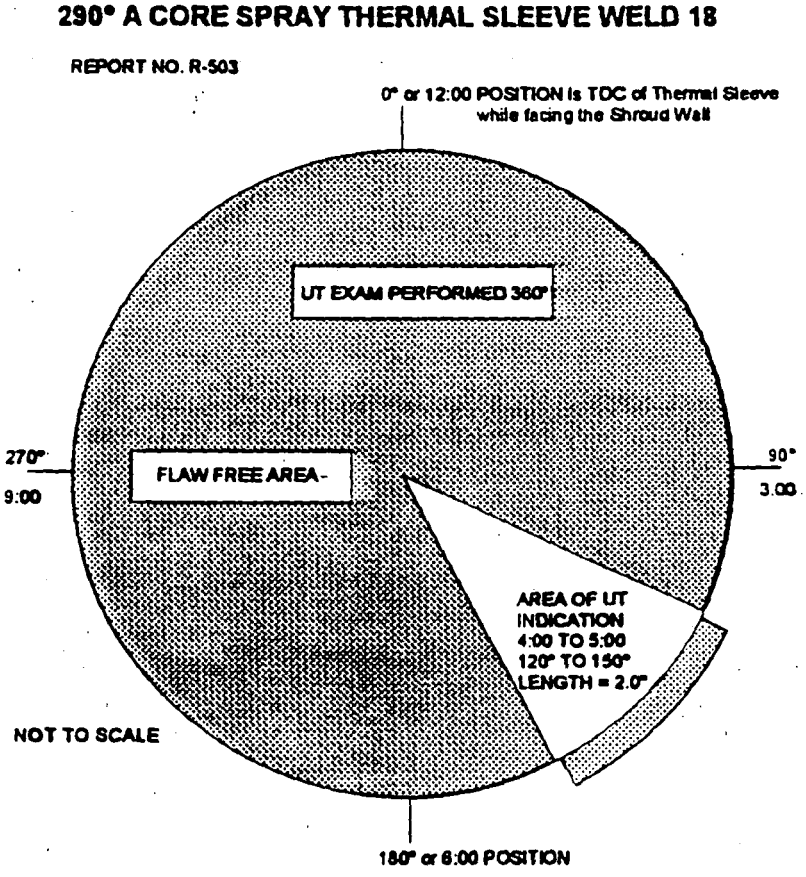

Figure 2.3 Ultrasonic Testing Examination Area And Flaw Location Thermal Sleeve Weld 18

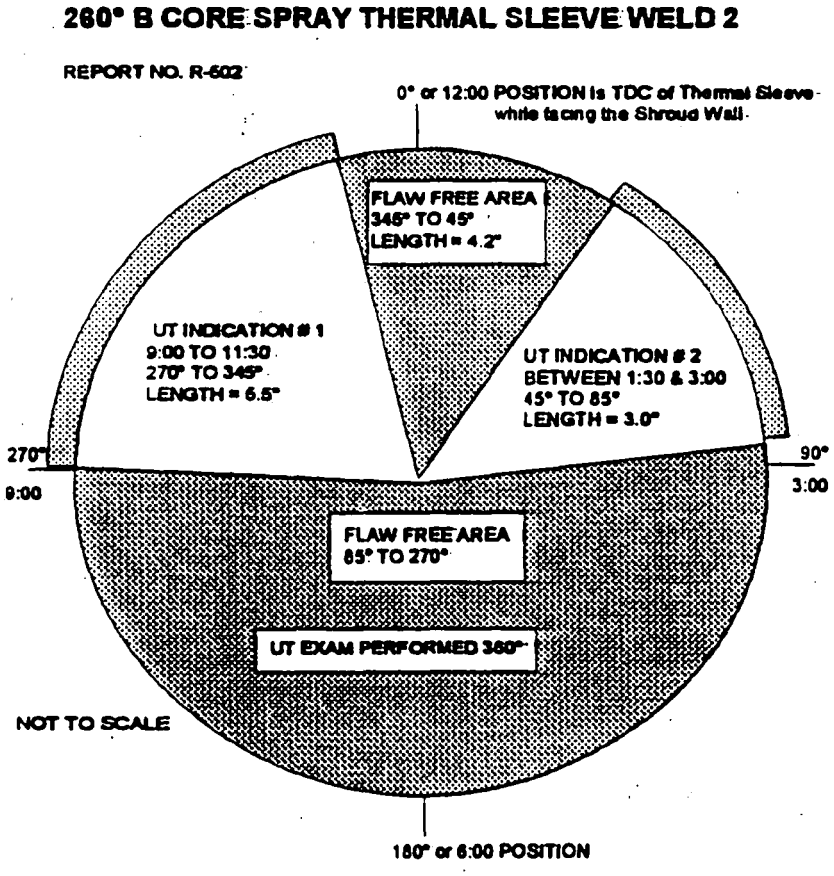

Figure 2.4 Ultrasonic Testing Examination Area And Flaw Location Thermal Sleeve Weld 2

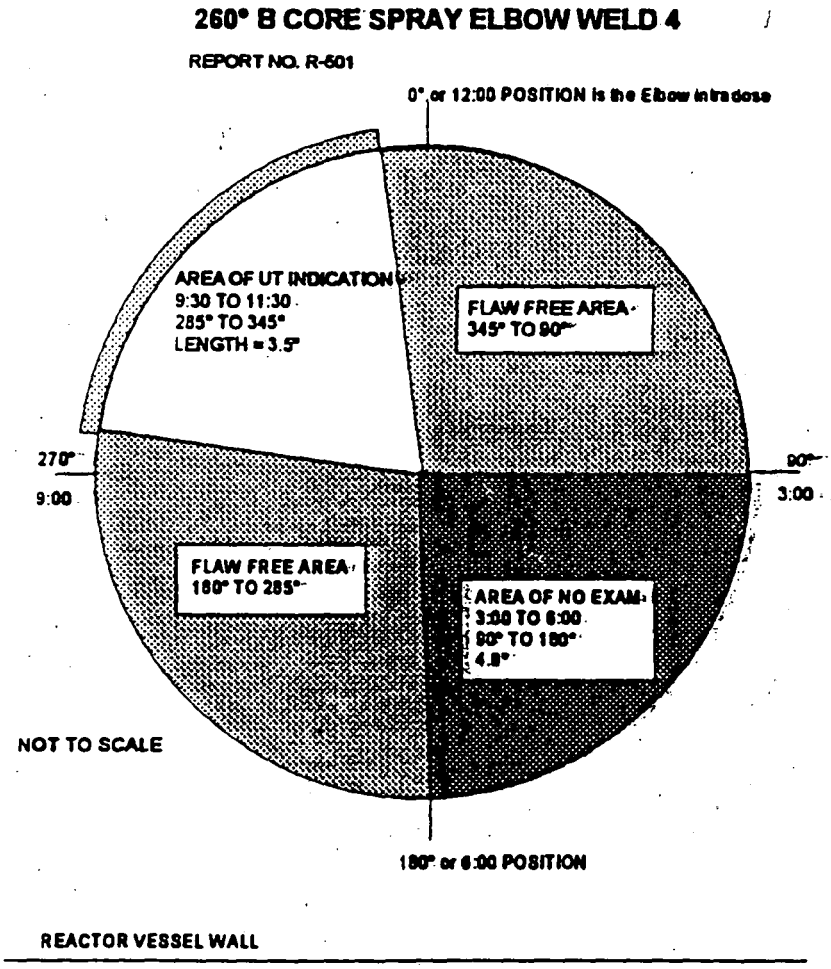

Figure 2.5 Ultrasonic Testing Examination Area And Flaw Location Elbow Weld 4

2.3 Crack Growth Length

The flaw lengths as determined by the VT and UT examinations were increased by a crack growth length to establish the evaluated flaw length (EFL). A crack growth length for an evaluation period of a 21 month hot operating cycle with a 90% availability factor was added to both ends of the flaw. A summary of the flaw lengths evaluated is provided in Table 2.1.

Table 2.1 Summary of Flaw Lengths

Flaw Location	Measured Flaw Length (Inches)[1]	Crack Growth Rate (Inches/ Hour)[2]	Crack Growth Length (Inches)[3]	Evaluated Flaw Length (Inches)[4]
A-Loop 290° Thermal Sleeve	2.00"	5.00 E-5	0.68"	3.36"
B-Loop 260° Thermal Sleeve	3.00" 5.50"	5.00 E-5 5.00 E-5	0.68" 0.68"	4.36" 6.86"
B-Loop 260° Inlet Elbow	3.50"	5.00 E-5	0.68"	4.86"

Notes:

1. Measured flaw lengths are the bounding results obtained from the VT and UT examinations.

2. 5.00 E-5 Inches/Hour represents an upper bound conservative industry limit for IGSCC crack growth in ductile material (Reference 18).

3. Crack growth is based on 13,608 hours of operation.

4. Evaluated Flaw Length (EFL) = Measured Length + 2(CGL)

3.0 MATERIALS EVALUATION

3.1 Overview

Cracks were found in the core spray loop A 290° upper sparger inlet thermal sleeve collar, the core spray loop B 260° lower sparger inlet thermal sleeve collar, and core spray loop B 260° lower sparger inlet elbow, (See Figures 2.1 and 2.2). A detailed review of the video tapes of all three crack locations revealed surface crack characteristics that were both jagged and branched. All of the cracks observed were initiated in the base material heat affected zones (HAZ). The thermal sleeve collar cracking appears to have initiated at the inside corner of the collar next to the collar to sleeve weld. The collar was machined from heavy wall tube resulting in a radius located in the HAZ, where large axisymetric residual stresses may be present. Consequently both the appearance and location of the cracking is consistent with Intergranular Stress Corrosion Cracking (IGSCC). This particular degradation mechanism is well documented for stainless steel components exposed to the high temperature reactor water of BWRs. Several other BWRs including Dresden Unit 3 and Quad Cities 1 have reported core spray piping cracks which were identified as IGSCC.

3.2 Fabrication

The General Electric Company (GE) design specifications as well as the fabricator records (Willamette) have been reviewed. All of the components are fabricated from solution heat-treated type 304 austenitic stainless steel ASTM A-312, Grade TP-304. The sleeve and collar tubing utilized heavy wall tubing that was machined to produce the desired shape. Records indicate the elbow weld was fabricated with the Gas Tungsten Arc Welding (GTAW) process. The thermal sleeve collar weld was fabricated with a GTAW root with Shielded Metal Arc Welding (SMAW) fill. The filler metal used for the SMAW was E308.

3.3 Crack Growth Rate

The principle driving force propagating IGSCC cracks comes from the weld residual stresses, because applied loads during normal operation are insignificant. The residual stresses are self-relieving and will diminish as the crack extends. As the stress intensity at the tip of the growing crack drops below the threshold stress intensity for IGSCC (K_{IGSCC}), crack extension will

stop. Therefore, the existing crack will propagate only as long as the residual stress field is sufficiently high to support crack propagation. The crack driving force may also be reduced by the change in the environment due to the adoption of hydrogen water chemistry in 1983. These arguments suggest that a lower IGSCC crack growth rate may be justified. However, ComEd has used the currently accepted bounding crack growth rate of 5.00×10^{-5} inches/hour (Reference 18).

3.4 Material Behavior

The ductile or brittle response of the material of cracked core spray components is evaluated with respect to initial characteristics and environmental degradation. All of the materials used in fabrication, were austenitic stainless steels as indicated in Section 3.2 of this report. These materials do not undergo phase transformation during thermal processing. The most significant material response to thermal processing is grain boundary precipitation of chromium carbides, and this response produces a zone adjacent to the grain boundaries that is depleted in chromium. This condition is termed sensitization and can be produced during welding. This condition influences the electrochemical response of the material (increasing susceptibility to IGSCC), but does not alter the ductility or toughness of the material.Exposure of austenitic stainless steels to irradiation can lead to a loss of ductility and an increased sensitivity to Irradiation Assisted Stress Corrosion Cracking (IASCC). The onset of IASCC occurs at approximately 5×10^{20} n/cm^2. The neutron fluence in the area of the core spray is less than 6×10^{18} n/cm^2, therefore, no reduction in toughness or increased sensitivity to IASCC is expected.

3.5 Conclusion

In conclusion, the cracking observed in the core spray system is the result of IGSCC in austenitic stainless steels. It has been shown in various tests that application of hydrogen water chemistry will slow the cracking to a rate that can be considered almost zero. Use of this water chemistry strategy to mitigate IGSCC has been in place at Dresden Unit 2 since 1983. The improved water chemistry coupled with the fact the stresses driving the cracking are residual stresses (self relieving) indicates that the rate of crack growth will be exceedingly slow. Therefore, the crack growth rate of 5×10^{-5} inches/hour represents a conservative upper bound limit. In addition, the material properties of the core spray system will remain ductile throughout the life of the system.

4.0 LOAD DEFINITIONS AND LOAD COMBINATIONS

4.1 Load Cases

DWGT = Dead Weight
TH01 = Thermal 1 (Normal Operation Differential Thermal)
TH02 = Thermal 2 (Core Spray Injection Differential Thermal)
TH03 = Thermal 3 (Upset Thermal Transient Differential Thermal)
P_1 = Pressure 1 (Internal Piping Pressure - Normal = 0 PSID)
P_2 = Pressure 2 (Internal Piping Pressure - Injection Mode = 47PSID)
P_3 = Pressure 3 (Internal Piping Pressure - Injection Mode = 64PSID)
DWH1 = Drag Load 1 (External Drag Loads on the Pipe Surface - Normal Flow)
DWH2 = Drag Load 2 (External Drag Loads on the Pipe Surface - Recirculating Line Break Flow)
DWH3 = Drag Load 3 (External Drag Loads on the Pipe Surface - Main Steam Line Break Flow)
OBDX = X Direction OBE Differential Seismic Displacement
OBDZ = Z Direction OBE Differential Seismic Displacement
OBDY = Y Direction OBE Differential Seismic Displacement
OBXY = X Direction OBE Response Spectra Analysis Plus Y (Vertical)
OBYZ = Z Direction OBE Response Spectra Analysis Plus Y (Vertical)
SSDX = X Direction SSE Differential Seismic Displacement (2 x OBDX)
SSDZ = Z Direction SSE Differential Seismic Displacement (2 x OBDZ)
SSDY = Y Direction SSE Differential Seismic Displacement (2 x OBDY)
SSXY = X Direction SSE Response Spectra Analysis Plus Y (Vertical)
SSYZ = Z Direction SSE Response Spectra Analysis Plus Y (Vertical)
SDIS = RRLB Core Shroud Displacement

4.1.1 Dead Weight (DWGT)

The core spray piping from the RPV nozzle to the shroud penetrations consists of 6" nominal Outside Diameter (OD) schedule 40 pipe and 8" nominal OD schedule 40 pipe. The piping is normally below the water level except for a LOCA event. In a LOCA event, the water level may drop below the core shroud penetrations. The weight of water contained inside the piping is included and the buoyancy force is conservatively neglected.

4.1.2 Thermal Expansion & Pressure Loads (TH01, TH02, TH03, P1, P2 & P3)

The radial and longitudinal differential thermal expansions of the RPV and the shroud are included in the thermal expansion analyses for the core spray piping. The radial dilation of the RPV under internal pressure is also considered for each thermal mode. The system temperatures and pressures were obtained from References 5 through 10.

Normal condition (TH01)

Temperature of the RPV section within the annulus region is 522°F which is the temperature of Region B as specified in the Reactor Thermal Cycles diagram. The temperature of the shroud (536°F) is taken as the average temperature of the annulus region and core region water temperature (550°F). Core spray piping temperature is the same as the temperature of Region B.

Emergency Shutdown, Core Spray Injection (TH02)

Per Dresden Technical Specification 3.2.2, during a plant emergency shutdown in a LOCA event the core spray system starts injection when the PRV pressure drops below 325 psig. At the beginning of the event, the RPV and the shroud remain at the normal operating temperature as given above, while the core spray piping contains cold water at 120°F. The reactor pressure drops rapidly to a pressure approaching 27 psig. The core spray piping temperature is the average temperature of the outside saturated temperature of 270°F at 27 psig and the inside cold water temperature of 120°F from the suppression pool.

Feedwater Transient Condition (TH03)

Per the Dresden Technical Specifications, a Loss Of Feedwater Pumps (LOFP) is considered for upset conditions. In this event, the water temperature in the annulus region is dropping rapidly to 300°F while the temperature of the RPV remains at the normal operating temperature of 522°F. The average temperature of the shroud under this transient condition is 433°F. The temperature of water inside the shroud is the normal operating temperature of 550°F. The temperature of the core spray piping is considered to be the temperature of the water in the annulus region.

4.1.3 Drag Load (DWH1, DWH2, DWH3)

The drag load of the reactor water on the core spray piping is evaluated in the normal operating condition (DWH1) and during a Reactor Recirculation Line Break (RRLB) condition (DWH2). The drag loads during an RRLB were found to envelope those of a Main Steam Line Break (MSLB). The RRLB event results in a 1/8" core shroud displacement in the direction of each Recirculation Suction Nozzle (155° and 335°).

4.1.4 Displacement Analyses (OBDX, OBDZ, SSDX, SSDZ SDIS)

The core spray piping is anchored to the core shroud at Node Points (NP) 307 and 327 as shown in Figure 5.1. It is attached to the RPV by supports located at node points 75, 125, 145 and 195. Displacement of the core shroud relative to the RPV results in differential support motion which is analyzed for OBE and SSE seismic events as well as for the RRLB and MSLB events. Two sets of core shroud displacements are analyzed for each of the seismic events. One set is based on the assumption of the core shroud remaining intact. The other set assumes a postulated circumferential break in the shroud at any horizontal weld location (cracked shroud). The bounding results based on the cracked shroud displacements were conservatively used for all flaw evaluations.

The seismic displacements are analyzed separately in the X and Z directions (Z = north-south axis, X = east-west axis). The vertical Y displacements are negligible. Since the SSE seismic displacements are twice the OBE displacements, only the OBE is analyzed and the results are doubled to obtain the SSE results.

The RRLB event was determined to bound the MSLB event with respect to loads on the core spray piping. It was analyzed by calculating the cracked shroud displacement in the direction of each recirculation suction nozzle at 155° and 335°

4.1.5 Seismic Inertial Analyses (SSEX, SSEY, SSEZ, OBEX, OBEY, OBEZ)

OBE 1% damping and SSE 2% damping were used in the piping analyses. The OBE 1% analysis results are obtained by using SSE 1%

damping spectra and multiplying the output by 0.5 since the SSE spectra are 2 X OBE spectra for the Dresden plant. Two spectra, one at the RVP penetrations and one at the core shroud penetrations are enveloped for this analysis. The core shroud response spectra used for this analysis was generated from an envelope of the shroud seismic responses to cracked circumferential welds at any combination of horizontal weld locations.

A uniform acceleration of .067g's (OBE) and .134g's (SSE) was used in the vertical Y - direction for all frequencies. The maximum of the X+Y or Y+Z combined seismic responses are used. The X-direction seismic displacement is combined with the "X+Y" inertial seismic. The Z - direction seismic displacement results are combined with the "Y+Z" inertial seismic results. Y-direction seismic displacements are negligible. The contributions of residual modal mass are included in the analysis results.

4.2. Load Combinations For Limit Load Flaw Evaluations

Normal & Upset (P = 0)
DWGT + DWH1
DWGT + DWH1 + OBXY
DWGT + DWH1 + OBYZ

Emergency and Faulted (P = 0)
DWGT + DWH1 + SSXY
DWGT + DWH1 + SSYZ
DWGT + DWH2
DWGT + DWH3

Beyond Design Basis Condition
DWGT + DWH2 + SSXY
DWGT + DWH2 + SSYZ
DWGT + DWH3 + SSXY
DWGT + DWH3 + SSYZ

Load Combinations For Leakage Evaluations (P= 47 and 64 PSID)

DWGT + TH02 + P2
DWGT + TH02 + P3

5.0 CORE SPRAY PIPING MODELLING AND ANALYSIS

The purpose of this piping analysis is to provide forces and moments on the 6" diameter core spray piping in the reactor annulus to be used for evaluation of cracks found in the pipe elbow and in the thermal sleeve collars of the core shroud penetration. The subject piping was analyzed using the PIPSYS program for the load conditions described in Section 4.0. The affected portion of the piping representing the upper and lower core spray spargers was analyzed utilizing two separate models delineated as the "upper sparger" and "lower sparger". The following two cases of seismic inertia anchor movement loads are evaluated for each model.

Case 1 - Cracked Shroud

The repaired core shroud is assumed to have 360° circumferential through wall cracking at any of the horizontal welds during the seismic event. The bounding relative displacements between the core shroud and vessel penetrations (NP's 307 and 327) are 1" in both the N-S and E-W direction for SSE, and 1/2" for OBE.

Case 2 - Uncracked Shroud

The current condition of the Dresden Unit 2 core shroud has remaining structural integrity of the circumferential welds and is considered to behave similar to an uncracked shroud. For this case (uncracked), the differential seismic displacements are 0.44" N-S and E-W for SSE and 0.22" for OBE. This case was determined to be bounded by Case 1 for the flaw evaluations.

5.1 Piping Models

The piping model is based on the design basis drawings (References 11 through 15) and is shown in Figure 5.1. It consists of core spray piping inside the reactor. From the 8" RPV nozzle and 8"X6" Tee-Box, the 6" piping follows the circumference of the reactor above the core shroud to two vertical legs which drop down and penetrate the core shroud horizontally after a 90° elbow. The model ends at these anchored shroud penetrations, NP 307 and NP 327. The piping is supported directly to the RPV at NP's 75, 125, 145, and 195.

This core spray piping exists in mirror image on both sides of the reactor, with the only difference being that one drops to a lower elevation on the core shroud to connect with the lower core spray sparger. The piping model for the lower sparger was modified by shortening the vertical legs to create the upper

sparger model. Since the two piping systems are 180° apart, the coordinate system used in the models points in opposite spatial directions for the two models. Isometric drawings in Figure 5-1 show the appropriate coordinate system. The piping is 6" Sch. 40, TP-304 stainless steel with a short leg of 8" Sch 40, TP-304 piping at the reactor nozzle. Flexible anchors are modelled at the core shroud penetrations with the model terminating at the 6" 90° elbow outlet. Stiffnesses for the penetration assembly were calculated based on the finite element analysis as described in Section 6.0. The 8"x6" tee-box is modelled as 8" Sch. 40 piping.

5.2 Lower Sparger Flexible Model

To evaluate the effects of crack compliance at the upper end of the 260° azimuth elbow of the lower sparger supply piping, a refined model was created to simulate the reduced stiffness of the cracked elbow. To accomplish this, a non-pipe element with a reduced moment of inertia about the weakened axis was inserted at the top of the elbow. This model was used to simulate a 60° circumferential pipe crack at the top of the elbow

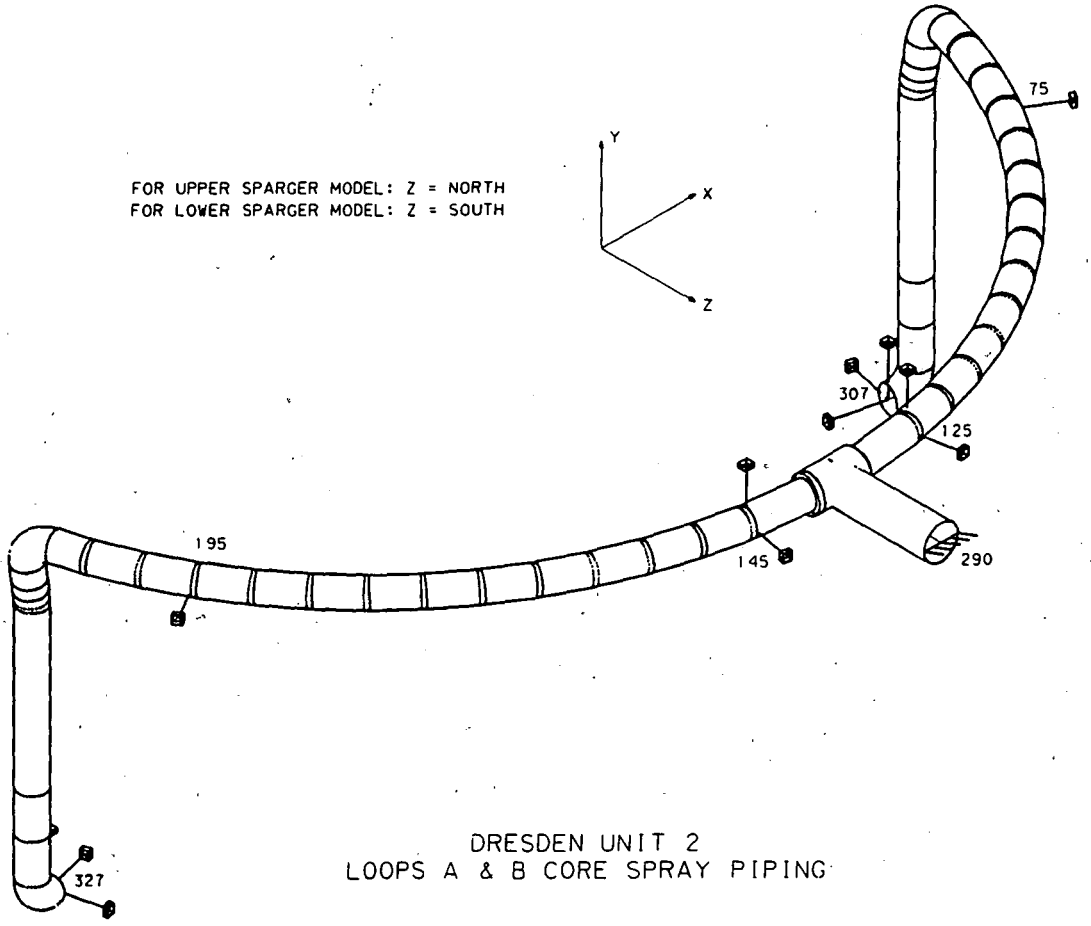

Figure 5.1 Core Spray Piping Analysis Model

5.3 PIPSYS Analyses Performed and Microfiche Index

Microfiche Run ID	Analysis Date	Description
Upper 6W	09-15-95	Upper Sparger Model - Cracked Shroud
Upper 6U	08-30-95	Lower Sparger Model - Uncracked Shroud
Lower 5W	09-15-95	Lower Sparger Model - Cracked Shroud Rigid Model[1]
Lower 5U	08-25-95	Lower Sparger Model - Uncracked Shroud Rigid Model
Lower 7W	09-15-95	Lower Sparger Model - Cracked Shroud 60° Flexible Model

[1]Flexible model incorporates reduced moment of inertia at cracked elbow. Rigid model assumes normal, uncracked pipe.

6.0 FINITE ELEMENT MODELLING AND ANALYSIS

6.1 Purpose/Objective

This section describes the finite element modeling and analysis (FEA) of the core spray shroud penetration assembly. The penetration assembly is located at the lower end of the core spray piping. The penetration consists of a 90^0 elbow, thermal sleeve, pipe and gussets welded to the shroud. A detailed description of the core spray piping and the penetration assemblies is given in the previous section and is illustrated in Figures 6.1 and 6.2.

The objective of the FEA is to determine the stiffness of the penetration assembly and the relative distribution of membrane forces between the thermal sleeve and the pipe penetration in the core spray shroud penetration assembly. The six stiffness values (3 translational and 3 rotational) were used for the PIPSYS piping analysis. The relative distribution of membrane forces between the thermal sleeve and the pipe penetration are used to assess the thermal sleeve cracks. The model was constructed and analyzed using the ADINA program (Reference 17). The model includes applicable portions of the pipe elbow, thermal sleeve, penetration pipe, gusset plates and as much of the shroud as is necessary to accurately determine the response of the penetration assembly to the overall core spray piping loads.

6.2 Model Description

The input data required to model the CS penetration assembly consists of geometry, material properties and loading. The geometry of the upper and lower penetration assemblies is shown on Willamette drawings (References 13 and 14) and is summarized below.

- 6" sch. 40 pipe and 90° elbow
- 8" O.D. tube for thermal sleeve, thickness = 3/16", connected to the pipe by 1/4" thick annular plate
- 5/8" thick gusset plates
- 2" thick shroud with a 6" by 4" thick ring beam at the top edge and at the lower edge supported by an annular plate; shroud inside radius = 108" and the height of the shroud above the top guide support plate is 33"

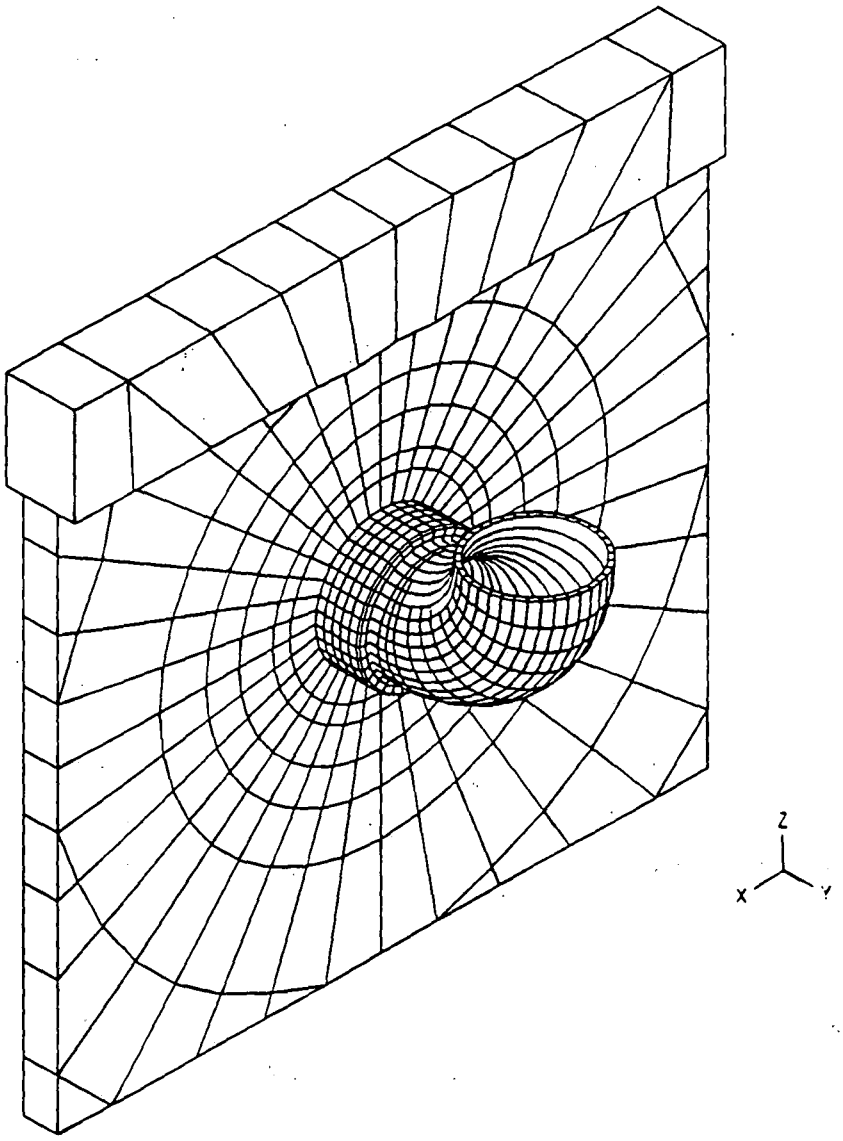

Figure 6.1 Three Dimensional View of FEA Model

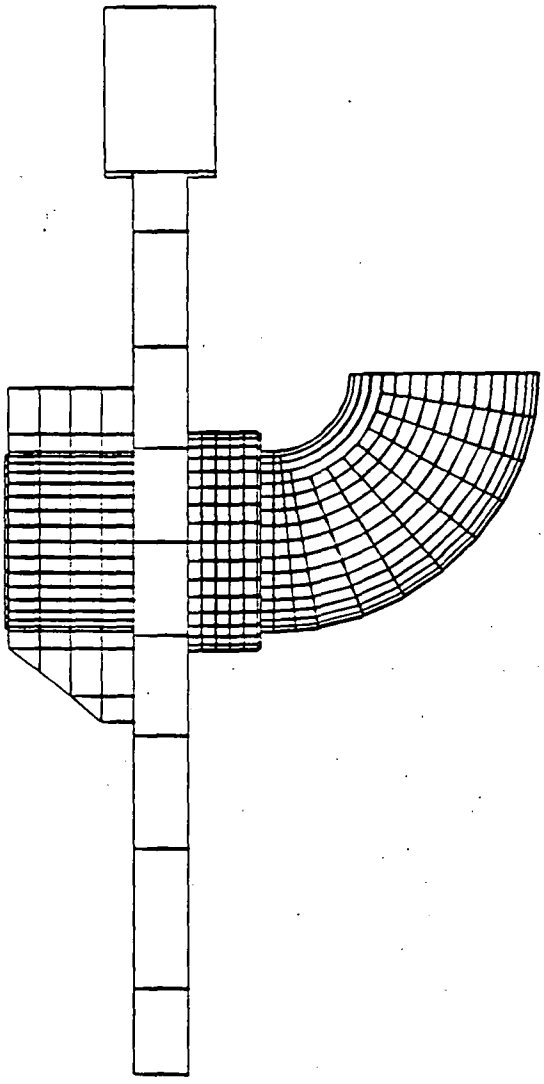

Figure 6.2 Vertical Cross Section of FEA Model

The material is type 304 SS, with the following properties at the design temperature of 550^0 F.

- Young's modulus, $E=25.8x10^6$ psi
- Poisson's ratio, $\nu=0.287$

All welded connections are such that full transfer of force and moment is provided across the connection (i.e. no reduction in stiffness is applied at the welded joints). The loading applied on the penetration assembly model consists of 6 separate cases (3 forces and 3 moments).

The elbow, pipe, sleeve, gussets and shroud are modeled by four-node quadrilateral shell elements. This is a non-flat (nodes need not be co-planar) general shell element for linear and non-linear analyses and is applicable to the analysis of thick and thin shells. A three dimensional view of the model is shown in Figure 6.1 as well as a vertical cross section in Figure 6.2. The cartesian global system of coordinates is located at the center of the 90^0 elbow. The circumferential pipe nodes are spaced at 10^0 angles, giving a total of 36 equally spaced nodes and 36 elements. Components of the penetration assembly were modelled at the midsurface of the component. Most of the model was generated using local cylindrical system of coordinates placed along the centerline of the elbow and pipe. Triangular (3-node) shell elements were used only when absolutely necessary and only in areas of the shroud which are far removed from the pipe to shroud interface.

6.3 Loading

The location at which stiffnesses are needed for the piping analysis is the lower end of the 90^0 elbow. Accordingly, the loads were applied at the node located at the center of the cross-section at the lower end of the elbow. In order to evenly transfer the load from a node at the center of the section to the pipe, the corresponding nodes on the circumference of the pipe are linked to the node at the center. Six analyses were made to determine six stiffness values (3 translational and 3 rotational). The six loads were applied incrementally as follows:

- for X-translational stiffness, load $P_x=2.0$ kip applied in two equal increments

- for Y-translational stiffness, load P_y=2.0 kip applied in two equal increments
- for Z-translational stiffness, load P_z=1.0 kip applied in one increment
- for X-rotational stiffness, moment M_x=100 in-kip applied in 5 increments, with half of moment applied in the first increment and the other half in 4 equal increments
- for Y-rotational stiffness, moment M_y=100 in-kip applied in two equal increments
- for Z-rotational stiffness, moment M_z=100 in-kip applied in two equal increments

6.4 Analysis and Results

Six separate analyses were performed to determine the stiffness and load distribution for each analysis case. Because of the presence of compression-only (gap) elements each analysis is nonlinear. Accordingly, an iterative method is used to solve the resulting nonlinear equilibrium equations. Also because of the nonlinearity aspect, the load is applied incrementally. The number of increments used to apply the final load in each case is defined in the previous section.

6.5 Summary of Results

The stiffness values at the lower end of the elbow are:

- k_x=4,156 kip/in for translation along X-direction
- k_y=2,127 kip/in for translation along Y-direction
- k_z=4,941 kip/in for translation along Z-direction
- k_{xx}=82,497 in-kip/rad for rotation about X-direction
- k_{yy}=179,252 in-kip/rad for rotation about Y-direction
- k_{zz}=53,993 in-kip/rad for rotation about Z-direction

The normalized (with respect to the load) distributions of moment load carried by the thermal sleeve collar are as indicated in Table 6.1.

Table 6.1 Normalized Load Distribution on the Thermal Sleeve Collar

Loading at the Pipe Anchor	Resulting Load on Thermal Sleeve
P_z = 1 kip	M_x = 0.69 in-kip
M_x = 1 in-kip	M_x = 0.238 in-kip
P_x = 1 kip	M_z = 1.13 in-kip
M_z = 1 in-kip	M_z = 0.43 in-kip
P_y = 1 kip	P_y = 0.388 kip

The stiffness values summarized above were utilized as a design input for the core spray piping model. The factors for axial and bending loads carried by the thermal sleeve were used to develop the loads for the flaw evaluations as described in Section 7.0 of this report.

7.0 FLAW EVALUATIONS

This section describes the methodology and details of the core spray line flaw assessments. The loading and stress analysis results as defined in the preceding sections serve as the primary inputs for these flaws evaluations. The flaw evaluations were performed using the ASME Section XI, Appendix C, limit load method for the flaws characterized in Section 2, and the material evaluation results presented in Section 3. The evaluation also includes an assessment of key analysis parameters and provides additional results based on the limits of these parameters.

7.1 Flaw Evaluation Methods

These flaws are evaluated using the limit load methodology of ASME B&PV Code Section XI, Appendix C, (Reference 19). This methodology assumes a plastic collapse failure mode of the flawed cross-section. Plastic collapse failure occurs when the remaining uncracked ligament is assumed to reach a plastic flow stress level and behaves as a hinge at failure (Reference 22). This failure mechanism is appropriate based on the inherent fracture toughness and ductility of type 304 austenitic stainless steels. As defined in ASME Section XI, Appendix C, the flow stress is defined as $3S_m$ at operating temperature. For these evaluations, the operating temperature is 550°F and the corresponding S_m is 16950.0 psi (Reference 20).

As previously stated the elbow flaw is located in the HAZ of a 100% GTAW weld. The thermal sleeve flaws are located in the collar adjacent to the collar to sleeve weld and are running circumferentially around the collar (see Figures 2.1 and 2.2). Consequently, these flaws, which are located in the HAZ of a non-flux weld and in the thermal sleeve collar base metal were evaluated using the base metal and GTAW evaluation formulas.

7.1.1 Flaw Characterization

As previously described in Section 2, the flaws being evaluated were found through a visual examination and corroborated by additional UT examinations. The UT examinations confirmed the existence and location of flaws that are believed to be connected to the inside surface of the elbow and collars. The UT examination method was able to confirm the location of the flaws identified visually, as well as identify an additional flaw believed to be connected to the inside surface of the Loop B thermal sleeve collar at 260°. Although the UT examination was capable of

determining the existence of internal and external surface flaws, it was not able to determine whether or not they were connected through wall. For conservatism, these evaluations assume the flaws to be through wall. As previously defined in Section 2, the evaluation period has been defined as a 21 month operating period with 90% availability. The crack growth during this period is based on the conservative IGSCC rate of 5×10^{-5} in/hr as defined in Section 3. The thermal transient and expansion loads associated with the start-up/shutdown and normal operation of the vessel are insignificant. During normal operation, the internal and external line pressure is equal. This eliminates any fatigue concerns associated with pipe line pressure fluctuations. Based on the low flow velocities and the horizontal rigidity (high fundamental frequency) of the core spray lines, flow induced vibrations will be negligible. Consequently, fatigue crack growth will not contribute significantly to crack extension and is not considered in the projected flaw length.

7.1.2 Flaw Evaluation Stress Inputs

The loads used in these evaluations were obtained from the piping model of the core spray lines including the detailed finite element model of the thermal sleeve shroud penetration assembly. These models generated the axial forces and bending moments acting on these flaws for the following loads:

- Weight
- Thermal
- Seismic
- Operating Drag
- LOCA

The design basis load combinations were evaluated and the worst case normal/upset and emergency/faulted condition load combinations were used for these evaluations. Additional beyond design basis, faulted load combinations were also evaluated to assess the design margin for these extreme cases. The simultaneous occurrence of a seismic SSE event with the RRLB LOCA was postulated as the bounding beyond design basis load combination. Reference 21 has determined that the RRLB LOCA event produces loads which bound the MSLB LOCA loads for this piping.

The loads used for the elbow flaw evaluation are taken directly from the piping analysis results reported in Section 5. The loads used for the thermal sleeve collar flaw evaluations were developed from the results of the finite element analysis of the thermal sleeve assembly. The finite element analysis of the thermal sleeve assembly was used to define the equivalent anchor stiffness of the assembly for the piping analysis model. Using the loads calculated in the piping analyses for the upper and lower core spray loops, additional thermal sleeve finite element analyses were used to determine the forces acting on the flaws.

Table 7.1 presents the membrane and bending stress values for the bounding design basis load combinations. In addition to the design basis load combinations, the additional faulted load combination of SSE and RRLB LOCA was examined to calculate, "beyond design basis" margins.

Table 7.1 Flaw Evaluation Stress Values (psi)

Flow Location	Design Basis (1)		Beyond Design Basis	
	σ_m	σ_b	σ_m	σ_b
Loop B 260° Elbow	25	713	25	954
Loop B 260° Collar	18	394	18	502
Loop A 290° Collar	17	392	17	475

(1) Includes the bounding load combination for normal/upset as well as emergency/ faulted conditions.

7.1.3 Flaw Limit Load Evaluations and Results

The allowable bending stress, P_B, for the limit load evaluation was calculated using equation 7-1.

$$P_B = 6 \frac{S_m}{\pi} \{2 \sin(\beta) - \frac{a}{t_n} \sin(\theta)\} \qquad (Eq.7-1)$$

$$with \quad \beta = \frac{1}{2} \{\pi - \frac{a}{t_n} \theta - \pi \frac{P_m}{3S_m}\}$$

$$and \quad \theta + \beta \leq \pi$$

Where θ is defined as the half angle as presented in Figure 7.1, and P_M is the membrane stress acting on the flaw. Because the flaws are assumed to be through-wall, the a/t_n ratio is equal to 1.

For these evaluations, the applied bending stress, P_{AB}, must be less than the allowable bending stress. The applied bending stress is calculated using equation 7-2.

$$P_{AB} = SF (P_m + P_b) - P_m \qquad (Eq. 7-2)$$

The code safety factor (SF) is 2.77 for normal/upset and 1.39 for emergency/faulted conditions. P_M and P_B are the applied membrane and bending stress, respectively.

The flaw evaluations were performed to determine the load margin for the end of evaluation period flaw size reported in Section 2. The load margin is defined as the ratio of the maximum permitted stress P_B, to the applied stress P_{AB}. This ratio represents the margin with respect to the applied load above the ASME Section XI safety factors. In addition to the load margins, the remaining months of operation were determined by calculating maximum flaw lengths which would meet the code required

safety factors. The months of operation required to reach the critical flaw length were calculated using the bounding crack growth rate of 5×10^{-5} inches/hour. The results of these calculations are presented in Table 7.2.

Table 7.2 Flaw Evaluation Results

Flaw Location	Load Margin Factor at end of Evaluation Period(1)		Months of Operation to Reach Critical Flaw Length	
	Design Basis	Beyond Design Basis	Design Basis	Beyond Design Basis
Loop B 260° Elbow	38	28	181	175
Loop B 260° Collar	41	33	127	123
Loop A 290° Collar	90	75	262	259

(1) This is the margin on load above and beyond the ASME Code Safety Factors of 2.77 for Normal/Upset conditions and 1.39 for Emergency/Faulted Conditions

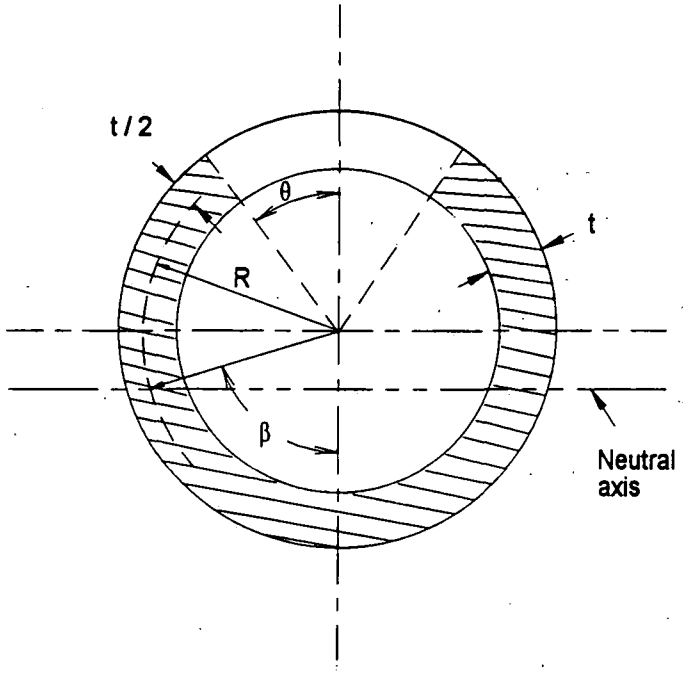

Figure 7.1 Cross Section of Flawed Pipe

7.2 Sensitivity Analysis

The most significant parameter influencing these flaw evaluations is the load acting on the flawed section. As previously discussed, the limit load method employed for this evaluation assumes a plastic collapse failure mechanism. Secondary or displacement controlled loads are relieved as the remaining ligament deforms plastically, thus the flaw evaluation is performed using only primary loads. The assumed plastic collapse failure mechanism is dependent on the material ductility and toughness, which is appropriate for type 304 austenitic stainless steels and non-flux welds. However, materials with reduced ductility and toughness such as flux welds, may exhibit ductile tearing with net section yielding, (i.e. an elastic-plastic failure mechanism). Since the thermal sleeve to collar welds are SMAW flux welds, this sensitivity analysis examines the impact of secondary loads and ductile tearing on the flaw structural integrity and remaining life estimates. The elbow flaw is located in the HAZ of a non-flux weld therefore, in accordance with the test results reported in References 23 and 24, and as specified in Section XI, Appendix C of the ASME code the greater material toughness and of ductility does not warrant an examination of the elastic-plastic failure mechanism. However, this sensitivity analysis examines the impact of the secondary loads on the elbow flaw structural integrity and remaining life estimates. The following evaluations determine the load margin for the end of evaluation period flaw size, from Section 2, and the remaining months of operation for the primary plus secondary loads.

7.2.1 Piping System Compliance

Examination of the piping analysis results confirms that the core spray piping in the RPV annulus is rigidly supported between the RPV wall and the core shroud. Consequently, the piping response to primary inertia and drag loads is small while the response to secondary, displacement controlled, loads is significantly larger. The magnitude of the loads generated from the differential movement of the core shroud and the RPV during thermal, seismic and LOCA events is dependent on the piping system flexibility. The system flexibility increases with flaw extension, therefore the magnitude of the secondary loads acting on the flaw are reduced. Figure 7.2 presents the results of a study which defined the load-deflection relationship for various flaw lengths (Reference 16). This figure demonstrates the increase in flexibility as a function of crack length.

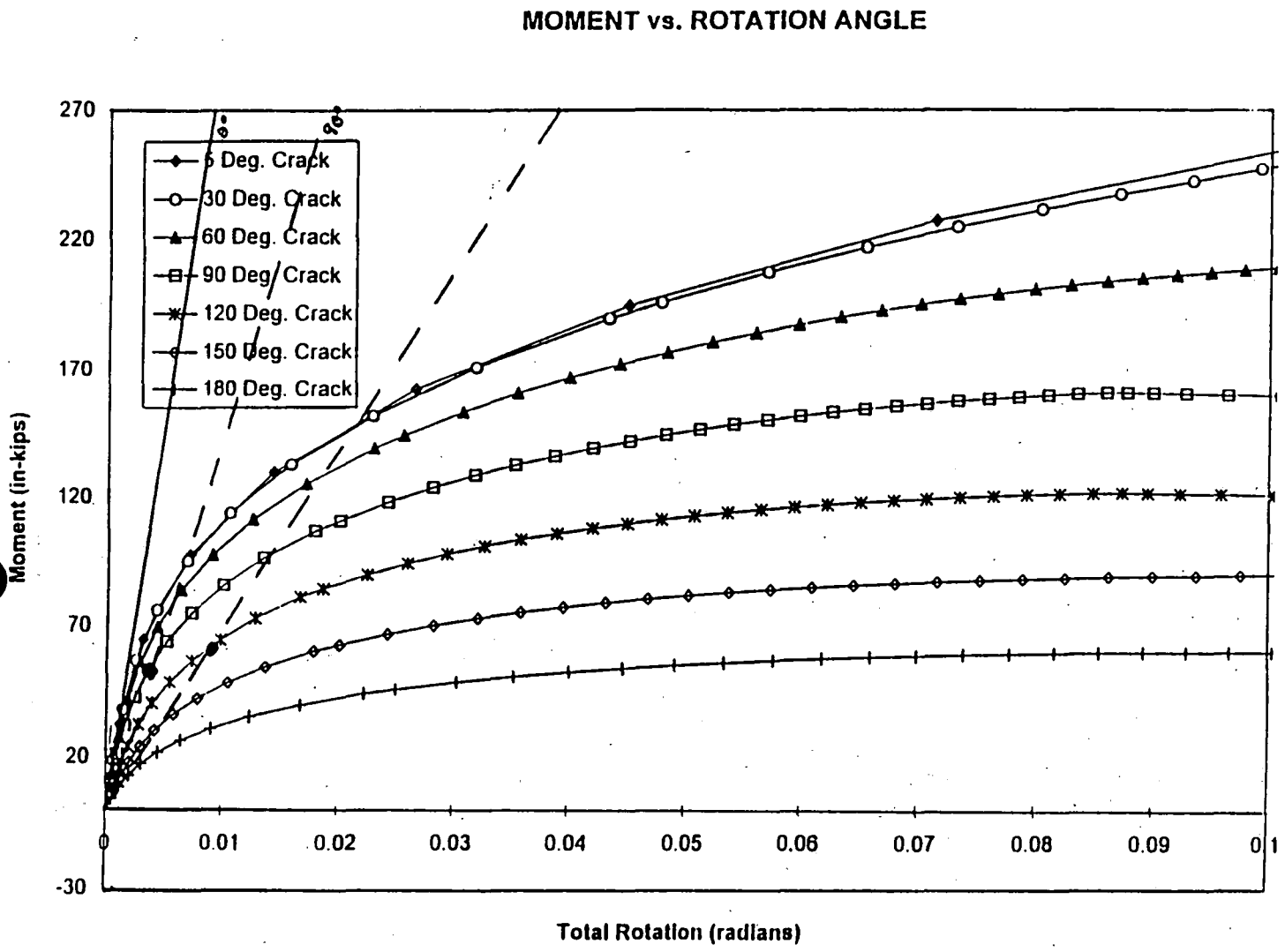

Figure 7.2 Moment - Rotation Angle Relationship

It conservatively used the material properties, i.e. stress strain data, of a flux weld. As previously described in Section 5, the rotational flexibility for an elbow flaw of 60° (3.3") and 120° (6.6") was included in the piping analysis model of the lower sparger, loop B. Because the only flaw in the upper sparger, loop A, was in the thermal sleeve collar, the flexibility of the piping analysis model was not changed. The loads from the lower sparger, loop B, model with the 60° flaw flexibility were used for these sensitivity evaluations.

7.2.3 Flaw Sensitivity Evaluations and Results

The loads used in these sensitivity evaluations are defined in the same manner as described in section 7.1. Table 7.3 presents the membrane and bending stress values for the bounding design basis load combination as well as the "beyond design basis" load combination.

These evaluations were performed using the simplified elastic -plastic approach defined in Section XI, Appendix C of the ASME B&PV Code. This approach requires that secondary stresses be included in a limit load formulation which uses a reduction factor, Z_1, to conservatively approximate an elastic-plastic failure mechanism. The allowable bending stress, P_B, for these evaluations was calculated using equation 7-1. However, the applied bending stress is modified, as stated above, to include the Z_1 factor for a SMAW weld and the secondary stresses as presented in equation 7-3.

$$PAB = Z_1\ SF(P_m + P_b + P_e/SF) - P_M \qquad \text{(Eq. 7-3)}$$

Where Pe is the applied secondary load bending stress, Z_1 is defined as

$$Z_1 = 1.15(1+0.013(OD-4))$$

For SMAW welds OD is the nominal outside diameter of the pipe, and the remaining terms are defined in equation 7-2. For the elbow flaw evaluation, the Z_1 factor is equal to 1.0.

The results of these sensitivity evaluations are presented in Table 7.4. It contains the load margins and remaining months of operation as defined in section 7.1.3. These results demonstrate that, for the limiting loads and material conditions, the structural integrity of the flaws is assured.

7.3 Flaw Evaluation Conclusions

Based on the results presented in Table 7.2, the minimum design basis load margin for the end of evaluation period flaw size is 38 and would require 181 months of operation to reach a critical flaw size. For the additional load combination of RRLB LOCA plus an SSE, which is beyond the design basis of the Dresden Station, the minimum load margin is 28 and would require 175 months of operation to reach a critical flaw size. These results demonstrate that the flaws, projected to grow at a conservative IGSCC crack growth rate of $5x\ 10^{-5}$ inches/hour for 13,608 hours, will remain structurally stable when subjected to design basis accident conditions. These results also demonstrate that reactor operation for more than 127 months can occur before the flaws are predicted to reach a critical length.

Table 7.3 Flaw Evaluation Sensitivity Analysis Stress Values (psi)

Flow Location	Load Type	Design Basis (1)		Beyond/Design Basis	
		σ_m	σ_b	σ_m	σ_b
Loop B 260° Elbow	Primary	25	573	25	802
	Secondary	114	11,550	130	12,976
Loop B 260° Collar	Primary	18	416	18	522
	Secondary	104	2,078	110	2,185
Loop A 290° Collar	Primary	17	392	17	475
	Secondary	130	2,501	140	2,690

(1) Includes the bounding load combination for normal/upset as well as emergency/faulted conditions.

Table 7.4 Flaw Evaluation Sensitivity Analysis Results

Flaw Location	Load Margin Factor at end of Evaluation Period (1)		Months of Operation to Reach Critical Flaw Length	
	Design Basis	Beyond Design Basis	Design Basis	Beyond Design Basis
Loop B 260° Elbow	3.0	2.6	100	93
Loop B 260° Collar	7.0	6.4	79	76
Loop A 290° Collar	12.9	11.8	209	206

(1) This is the margin on load above and beyond the ASME Code Safety Factors of 2.77 for Normal/Upset conditions and 1.39 for Emergency/Faulted Conditions

8.0 LEAKAGE FLOW EVALUATIONS

This leakage flow evaluation determines the rate that water is lost from the elbow flaw in the lower sparger, loop B, during core spray injection. This evaluation does not evaluate leakage from the two thermal sleeve collar flaws because these are not part of the core spray pressure boundary and leakage from the collar flaws does not contribute to core spray system leakage. The core spray system leakage is calculated for elbow flaw lengths at the end of the evaluation period, as reported in Section 2, and at the end of life.

8.1 Leakage Calculation Methodology

The elbow flaw leak rate is calculated using the PICEP program developed by EPRI for Leak-Before-Break applications, (Reference 25). This program uses elastic-plastic fracture mechanics to calculate the crack opening area of a through wall circumferential flaw. It calculates the leak rate based on "Henry's Homogeneous Nonequilibrium Critical Flow Model" (Reference 26). This evaluation is based on the combined membrane and bending stresses acting on the flaw from the combined loads which occur during the injection mode. The Ramberg-Osgood stress-strain parameters were obtained from Reference 27, the IPIRG Task 1.3 piping system tests database developed by Batelle, and are an average of type 304 base metal tests at 550°F and 70°F. Because the piping temperature cools very quickly during the LOCA event and after the initiation of the core spray flow at 120°F, the line temperature is reduced to an average temperature of 195°F for this leakage calculation. Interpolation of the stress-strain data for 550°F and 70°F to 195°F was used to establish the stress-strain input to the leakage calculations.

8.2 Leakage Calculation Applied Loads

During the core spray injection mode, the elbow flaw is subjected to the combined flow induced loads and differential thermal expansion loads. At approximately 60 seconds after a DBA LOCA, the core spray maximum differential pressure is 47 psid at a flow of 4600 gpm. As the reactor vessel pressure continues to reduce to 0 psig, the maximum differential line pressure would reach 64 psid at the core spray pump runout flow rate of 5350 gpm (which will occur at a time much later than the PCT which occurs at 169 seconds). The leakage flow rate was calculated for both the 47 psid and 64 psid line pressure conditions. The thermal load acting during the injection mode is conservatively based the core shroud and reactor vessel being hot

while the core spray piping is cold, as described in Section 4. This thermal loading is applied to the piping model which includes the flexibility of a 60° flaw which is the current size of the flaw without considering IGSCC crack growth. This produces conservative membrane and bending stresses which will decrease as the flaw grows.

8.3 Calculated Leakage

The leakage was calculated based on the previously described loads and material properties and presented in Figures 8.1 and 8.2 for an injection pressure of 47psid and 64 psid respectively. From Figure 8.1, the leak rate for the end of evaluation flaw size is 1.15 gpm and at the end of life is 70.22 gpm. From Figure 8.2, the leak rate for the end of evaluation flaw size is 1.38 gpm and at the end of life is 82.53 gpm. The end of life flow rates calculated here are based the conservative thermal stresses generated from a more rigid model. Since the end of life flaw length is significantly larger than the 60° flaw used in the piping model, the flexibility of the model could be increased, thus reducing the piping membrane and bending stresses and the corresponding leakage flows. The results of this leakage evaluation are compared to the system capacity in Section 9.0 of this report.

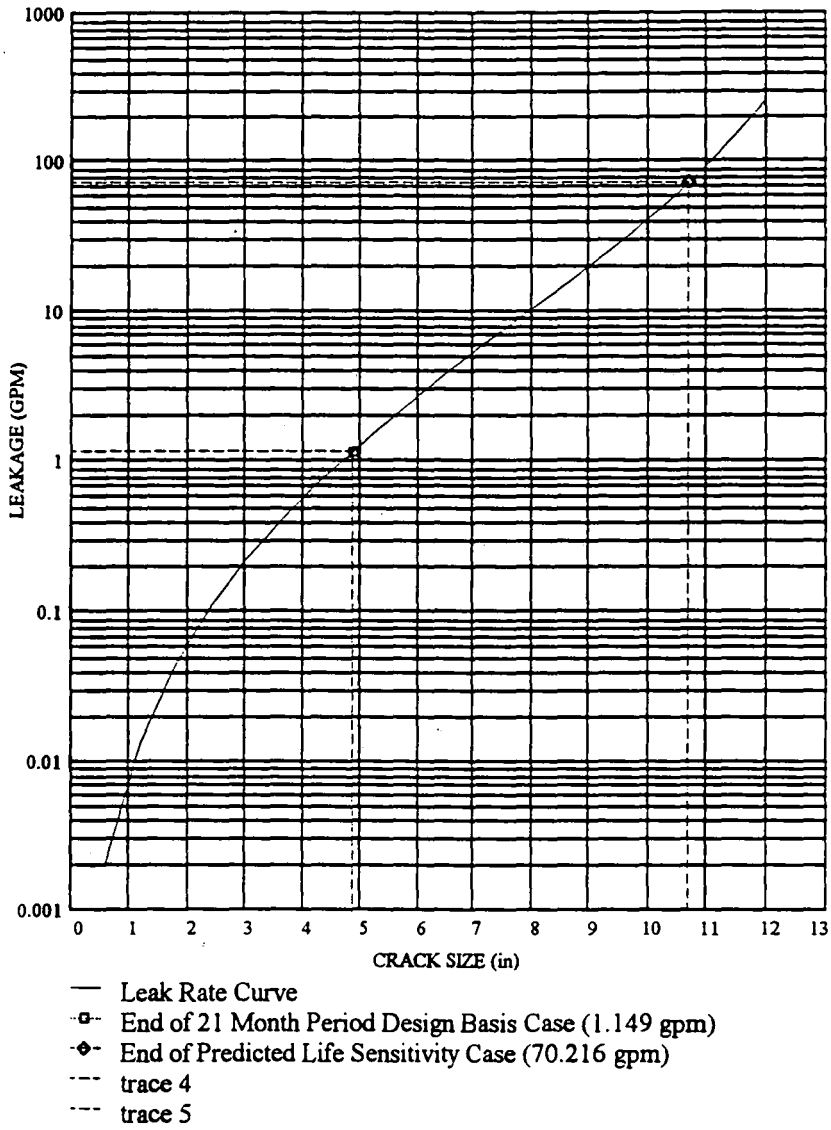

Figure 8.1 Leakage Rate at a Differential Pressure of 47psi

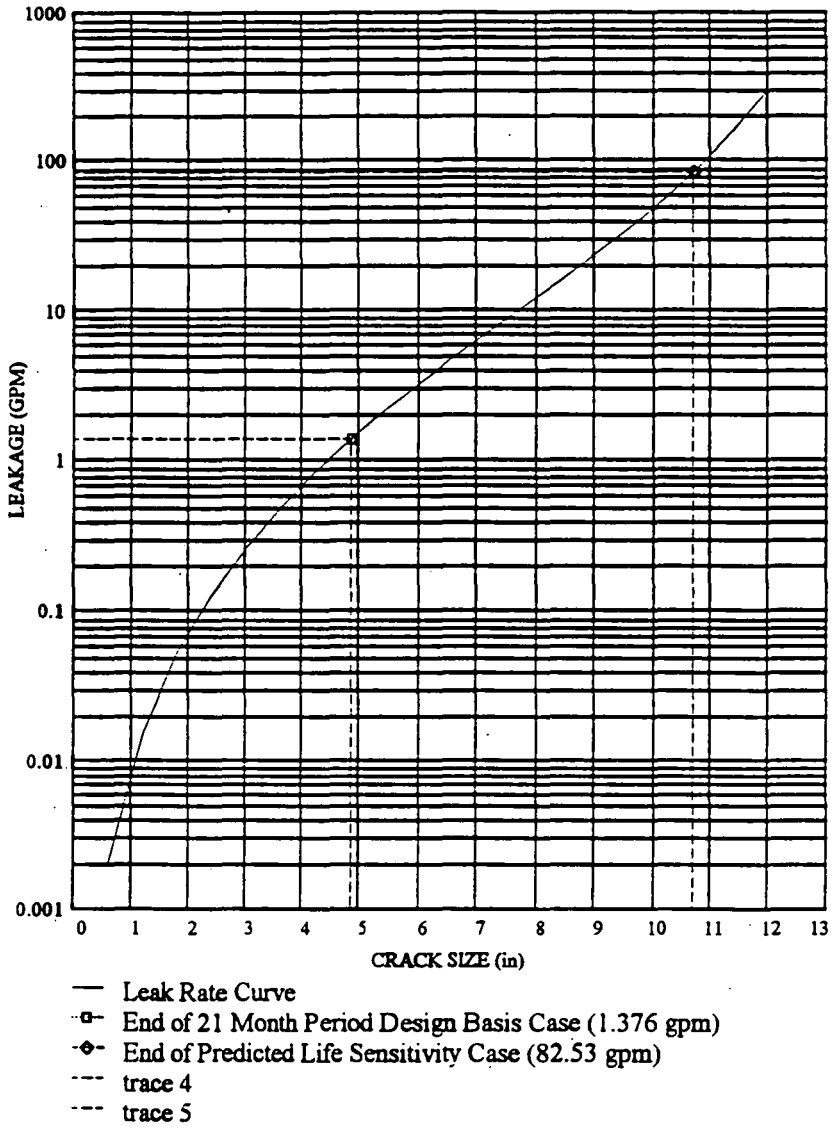

Figure 8.2 Leakage Rate at a Differential Pressure of 64psi

9.0 CORE SPRAY SYSTEM LOCA EVALUATION

9.1 Core Spray System Description

The core spray system along with High Pressure Coolant Injection (HPCI), Low Pressure Coolant Injection (LPCI) and Automatic Depressurization System (ADS) make up the ECCS for Dresden Unit 2. The core spray system consists of two independent redundant loops each consisting of a pump, valves, piping and independent circular sparger ring inside the core shroud just above the core. The normal water source for pump suction is the suppression pool. Each core spray pump takes suction from a common ring header that has four suction lines. A fill system is used to ensure that the core spray discharge lines remain pressurized. This fill system consists of a pump which takes suction from the suppression pool via a core spray suction line and discharges to the core spray and LPCI pump discharge lines. The power source for each core spray loop is located on an independent emergency bus. Each core spray loop is designed so that each component of the subsystem can be tested periodically.

9.2 Core Spray System Safety Function

Each core spray loop is designed to operate in conjunction with the LPCI subsystem and either the ADS or HPCI subsystems to provide adequate core cooling over the entire spectrum of liquid or steam pipe break sizes. For the small line break accident, the ADS or HPCI subsystems are used to depressurize the vessel to a point where the core spray and LPCI systems can be initiated in time to ensure adequate core cooling. For the large break LOCA, the depressurization assistance from HPCI or ADS is not required. For the full range of LOCA break sizes, the current design basis requires that core cooling be provided by both core spray loops operating together or by one core spray loop operating with two LPCI pumps (one LPCI subsystem). The core spray loops can be powered from either offsite or onsite sources.

9.3 Leakage Flow Evaluation

The bounding case for core spray is the DBA-LOCA consisting of a reactor recirculation suction line break in combination with a single failure of the LPCI injection valve. This requires core spray to cool and reflood the core without assistance from LPCI.

The critical DBA-LOCA leakage is based on the maximum core spray flow of 4600 gpm and is 1 gpm through the elbow flaw. This is based on a flaw length developed after 21 months of operation at 90% availability with crack opening based on the design basis load combinations. A bounding leakage of 70 gpm was determined based on the end of life flaw size and the design basis load combinations. The flaws in the two collars are not part of the core spray system pressure boundary, are located above 2/3 core height and thus do not factor into the core spray system leakage evaluation.

During the blowdown phase of the DBA-LOCA, any core spray flow due to leakage in the annulus piping will be lost through the break. This volume of water loss can be directly subtracted from the core spray flow assumed in the current DBA-LOCA calculations. This would cause a decrease in liquid flow to the lower plenum during the reflood phase of the DBA-LOCA and a subsequent increase in the time required to quench the "hot node". A preliminary estimate of the PCT increase is 36° F for a core spray leakage of 300 gpm. Linear interpolation can be used to estimate the change in PCT for leakages less than 300 gpm. Thus, the 1 gpm leakage will result in a negligible increase in the PCT. Assuming the maximum end of life flaw size with a leakage of 70 gpm, the PCT increase will be approximately 8° F.

The current DBA-LOCA calculation, which is based on 8x8 fuel, indicates the PCT is 2045° F. The actual installed fuel is Seimens 9x9. Preliminary calculations indicate that for 9x9 fuel, the PCT is less than 1950° F for a postulated leakage rate of 70 gpm.

Based on this evaluation the postulated leakage is not significant since the PCT would remain below 2200° F for the Seimens 9x9 fuel which is presently installed. Leakage resulting from the elbow flaw would only have an impact on the PCT for the postulated bounding case of a recirculation line break with concurrent loss of the LPCI system. Without the loss of LPCI, there would be no impact on the PCT.

10.0 SUMMARY AND CONCLUSIONS

Crack indications were identified at three locations on the core spray downcommers during the D2R14 in vessel visual inspections. This core spray line inspection was planned and implemented as part of a thorough rebaselining inspection of the reactor internals. The approach used to define and evaluate the flaws in the Dresden Unit 2 core spray downcommers was complete and thorough and addressed all relevant parameters. The approach was to fully utilize all of the latest industry and plant specific information to plan and execute the inspections as well as the engineering evaluations. This is reflected in the thorough and detailed visual inspections that were performed along with the use of ultrasonic testing to corroborate and clarify the inspection results. The stress analysis and flaw evaluations were performed using verified design inputs for all key analysis parameters. Where the analysis parameters were determined to have a significant impact on the analysis or evaluation, a conservative bounding value was selected and a sensitivity study was performed. Provided below is a summary description of the analyses and evaluations performed along with the conclusions reached.

The details of the visual and ultrasonic examination results are defined in Section 2 of this report. The critical flaw identified was a 3.5 inch long crack in the B-loop inlet elbow. This crack was conservatively assumed to be through wall and was extended using a bounding IGSCC crack growth rate of 5.0×10^{-5} for a 21 month operating cycle to a evaluated flaw length of 4.86 inches. The UT methodology developed and utilized as part of the flaw characterization was prequalified and independently verified by industry experts. The approach and methods used represent the best available in the industry and provide an accurate basis for performing a flaw evaluation.

The materials evaluation included a detailed assessment of the inspection records, the fabrication details, the key material behavior characteristics as well as a review of relevant industry information. The review of the inspection results and pertinent industry experience indicates that the flaws are the result of IGSCC. The fabrication records were reviewed as part of the determination of the cause of the cracking as well as to identify the appropriate material properties for the flaw evaluations. The review of the material behavior and other aspects provided corroboration of the conclusion that the flaws were IGSCC and thus a conservative crack growth rate was selected for the flaw evaluations. The results of the materials evaluation performed by the ComEd metallurgists were verified by an independent industry expert.

The flaw evaluation was precluded by a thorough and complete review of the applicable loads and load combinations for the affected piping. The latest design

basis information regarding RRLB, MSLB and Seismic loads were incorporated into the loads definition. A detailed piping analysis was performed for the defined loading conditions including several additional analysis cases associated with the flaw sensitivity study. The piping modelling included such details as the rotational stiffness properties of the penetration assemblies and the cracked piping. The results of the piping analysis represent an accurate and complete definition of the critical flaw section stresses under design basis and beyond design basis load combinations. The key analysis parameters associated with the loadings, material properties and system operating conditions were reviewed and enveloped by the analyses performed.

The flaw evaluations and sensitivity study were performed using the ASME Section XI, Appendix C limit load methods. The evaluations performed include an assessment of the key analysis parameters and provides results based on the limits of these parameters. The critical elbow flaw has a load margin under design basis load combinations of 38 times the ASME code factor of safety. The critical thermal sleeve collar flaw has a load margin under design basis load combinations of 41 times the ASME code factor of safety. The sensitivity study concluded that even with consideration of all of the upper bound limits of the analysis parameters a load margin of 3.0 times the ASME code safety factor exists for design basis load combinations. This load margin corresponds to an operating cycle length of 100 months with the upper bound crack growth rate prior to meeting the code specified factors of safety. These results clearly corroborate the conclusion that the core spray piping is very flaw tolerant and has sufficient margin to perform it's design basis function for the next operating cycle.

The leakage flow was calculated using the end of the operating cycle crack lengths in conjunction with the bounding flaw section stresses. The estimated leakage of 1 gpm for the system operating flow rate of 4600 gpm results in no significant increase in the peak cladding temperature (PCT). The leakage associated with the end of life crack size is 70 gpm resulting in an increase in the PCT of approximately 8° F. The effect of these changes in the PCT is insignificant and is well within the existing design basis margin. The combined assessment of the system structural margin as well as core spray system functional capacity confirm the conclusion that sufficient margin exists to operate for one cycle with the identified flaws. A reinspection of these flaws will be included in the IVVI plan for the D2R15 outage and will serve as the basis for continued monitoring of the cracking in the core spray system.

11.0 REFERENCES

1. BWR-VIP Report GENE-523-1113-0894, "BWR Core Shroud and Evaluation Guidelines", September 1994.

2. SL-4973 Revision 0, "Safety Assessment of Horizontal Core Shroud Welds H1 Through H7 for Cycle 14 Operation of Dresden Unit 2", December 12, 1994.

3. UT Examination Summary Sheet, Report No. R-500, "Dresden Unit 2 Core Spray", August 16, 1995.

4. August 9, 1995 Letter from G. Selby of EPRI NDE Center, to J. Whitman of ComEd, "UT Technique for Dresden Core Spray Piping".

5. GE Drawing 921D265, Revision 1, "Reactor Pressure Vessel Thermal Cycles".

6. GE Specification 21A1109, Revision 2, "Dresden Units 2&3 RPV Design Specification".

7. GE Specification 25A5688, Revision 2, "Shroud Stabilizer Hardware". Design Specification.

8. Dresden UFSAR Sections 6.2 and 6.3.

9. Siemens Report ANF-88-191, December 1988.

10. GE Drawing 161F310, Revision 1, "Process Diagram - Core Spray System".

11. GE Drawing 104R921, Revision 3, "Assembly - Reactor Nuclear Boiler".

12. GE Drawing 104R861, Revision 10, "Assembly - Reactor Nuclear Boiler".

13. Willamette Iron & Steel Co. Drawing E861 Sheet 1, Revision H, "Dresden 2 & 3 Core Structure, Shroud".

14. Willamette Iron & Steel Co. Drawing E861 Sheet 2, Revision B, Dresden 2 & 3 Core Structure, Shroud".

15. GE Drawing 885D660 Sheet 3, Revision 4, Dresden 2 & 3 Core Structure, Shroud".

16. SIA Calculation CECO-42Q-301, Rev. 0, "Compliance Study of Flawed Pipe".

17. ADINA R&D Inc. Manual for ADINA Program Version 6.1.

18. NUREG-0313, Revision 2,"Technical Report on Material Selection and Processing Guidelines for BWR Coolant Pressure Boundary Piping".

19. ASME B&PV Section XI Appendix C, 1989.

20. ASME B&PV Section III, Appendix I, 1989

21. Sargent & Lundy Calculation 9389-64-DQ.

22. "Evaluation of Flaws in Austenitic Steel Piping," EPRI NP-4690-SR, July 1986.

23. "Instability Predictions for Circumferentially Cracked Type - 304 Stainless Under Dynamic Loading," EPRI, NP-2347, April 1982.

24. "Degraded Piping Program Phase II, Semi Annual Report, October 1984 - March 1985," NUREG/CR-4082, BMI-2120, Vol. 2, July, 1985.

25. "PICEP: Pipe Crack Evaluation Program (Revision 1)," EPRI NP-3596-SR, Revision 1, December 1987.

26. "The Two-Phase Critical Discharge of Initially Saturated or Subcooled Liquid," Nuclear Science and Engineering, 41, 1970.

27. "Pipe Fracture Database," from Douglas A. Scarth, Task Group Chairman, ASME Section XI Task Group on Pipe Flaw Evaluation, October 21, 1992.

28. SL-5019 Revision 0, "Dresden Unit 2 Core Spray Flaw Evaluation Report", September 1995.

ATTACHMENT B

INTEGRATED EVALUATION REPORT OF CORE SPRAY FLAW REVISION 1